Synergism of blended extract of *Ageratum houstonianum* and *Chromolaena odorata* leaves on the corrosion inhibitor of reinforcing steel in concrete composite

Madhab Gautam[1,2], *Laxman* Gupta[1], *Nabin* Pandey[1], *Nootan Prasad* Bhattarai[1*], and *Jagadeesh* Bhattarai [1†]

[1]Central Department of Chemistry, Tribhuvan University, Kirtipur 44618, Kathmandu, Nepal
[2]Department of Chemistry, Tribhuvan M. Campus, Tribhuvan University, Tansen 32500, Palpa, Nepal

Abstract. Corrosive degradation of reinforcing steel (RS) in concrete composite (ConC) is a significant factor contributing to the early collapse of reinforced concrete infrastructures. The degradation of the RS in ConC impacts if appropriate corrosion control efforts are not applied promptly. Plant-based green extracts have been recently used as anticorrosive materials to prevent RS corrosion. This study investigated the effectiveness of various concentrations of blended extracts from the leaves of *Ageratum houstonianum* and *Chromolaena odorata* (referred to as AHL-COL) in controlling the corrosion of reinforcing mild steel (RMS) in the ConC using a half-cell potential measurement with the help of the ASTM C876-22b standard. Performed the surface analysis using scanning electron microscopy with energy dispersive X-ray spectroscopy (SEM-EDS) to examine the anticorrosive actions of the AHL-COL concentrations. The corrosion probability (P_{corr}) of the RMS in concrete beams with 500-2000 ppm AHL-COL is synergistically lowered compared with the control concrete beam or even the presence of individual plant extracts, as evidenced by shifting the corrosion potential (E_{corr}) to a zone where the P_{corr} of the RMS should be < 10%, and also supported by electron microscopic, and SEM-EDS analysis.

1 Introduction

Reinforced concrete (RC) is one of the most widely used nano-composite structural materials over the last two centuries [1]. One of the reasons for the early damage of RC structures is the corrosion of reinforcing steel (RS). The RS corrodes in concrete composite (ConC) when it is in contact with ingressed water/moisture, salt ions (chloride, sulfate, sulfide), oxides of nitrogen, H_2S, CO_2, among other substances, through the concrete mix [2]. The RS is passivated in ConC through the formation of Fe_2O_3, which functions as protective layer on the mild steel in the highly alkaline concrete solution with a pH 13±0.5. Even so, when chlorides, sulfates, CO_2, moisture, and so on ingress through the pores of the ConC to the RS surface, such protective passive film undergoes breakdown by a decrease in pH <10 [3]. As a result, the corrosion phenomena of the RS in ConC become noticeable.

The corrosive damage of the RS occurs due to the reduction of strength, durability, and elasticity, i.e., most mechanical properties [4]. Corrosion scientists also emphasized the need for a meticulous corrosion control mechanism of the RS in ConC [5], which not only provides a guarantee for the structure's durability and strength but also causes damage to the environmental and economic aspects. The corrosive damage of the RS is a source of the early destruction (i.e., less than 50 years) of concrete structures (ConS). The restoration cost of the corroded ConS is around 3% of the gross domestic product of the developed countries [6]. The cost of RS corrosion in ConC depends on the severity of such a critically polluted environment [7].

To overcome such RS corrosion-based concrete impairment, researchers have widely practiced adding low concentrations of various synthetic chemicals as corrosion inhibitors for the significant improvement of the quality control of the RC properties like corrosiveness, durability, stability, and so on. An effective plant-based corrosion inhibitor enhanced adsorption capacity on metal surfaces in aqueous electrolytes, biofuels and their blends. However, few works have reported on plant-based extracts as corrosion inhibitors in concrete electrolytes. In recent years, some research groups like Ahmed & Ganesh [8], Ghoreishiamiri *et al.* [9], Bhattarai *et al.* [10], and Valdez-Salas *et al.* [11] have focused on the use of plant-based phytochemicals as green additives in ConC to control the early corrosive damages of mild steel in the RC infrastructures.

* Corresponding author : neutan08@ygmail.com
† Corresponding author : bhattarai_05@yahoo.com

The plant-based green additives contain a wide range of phytoconstituents, which are highly basic with high electron density and heteroatoms such as N, O, P, and S, serving as active centers for the adsorption onto the RS surface [12]. The increasing order of inhibition potency of the heteroatoms follows the sequence O<N<S<P [13]. In general, the plant-based corrosion inhibitors passivate the RS in ConS in two ways- either by enhancing the formation of a protective oxide film through a de-electronation effector by selectively adsorbing on the metal surface and by generating a barrier film that prevents ingress of corrosive agents through the ConC to the RS surface [14].

The plant-based extract also contains π-electrons in heterocyclic ring compounds, which adsorb onto the RS surface [15], following these four steps: (i) electrostatic interactions between charge-carrying phyto-molecules and metal ions, (ii) interaction between vacant d-orbital of the metal atom and lone pair electrons of N, S, or O hetero-atom, (iii) interaction between unoccupied d-orbital of the metal atom and π-electrons of the aromatic ring compounds, and (iv) combination of the above-mentioned three processes [16]. Thus, imparting a passive film formation through physical, chemical, or both adsorption processes.

In the last seven years, abundant numbers of phyto-constituents, extracted from different plant parts [17] exhibited as a potent green inhibitor in aqueous electrolytes to prevent metals corrosion. A few Nepali plants' leaves have been utilized to prepare plant-based corrosion inhibitors, which act as anti-corrosive agents for controlling the mild steel corrosion in aqueous environments, fossil fuels, and their blends. However, most of them are limitedly employed as green-based corrosion inhibitors in ConC to control the early corrosion damage of the reinforcing mild steel.

Researchers have thoroughly focused their work on inhibiting the corrosion of steel in chloride-contaminated concrete pore solution using leaf-based extracts from *Fatsia japonica* [18], *Urtica dioica* [19], *and Platanus acerifolia* [20] plants. They possess desirable properties as green corrosion inhibitors, which include heteroatoms such as nitrogen, oxygen, and sulfur, as well as aromatic ring phyto-compounds like alkaloids, flavonoids, phenols, polyphenols, amino acids, tannins, and terpenes. These phyto-compounds act as effective anti-corrosive agents. The adsorption process of physical, chemical, or both between phyto-molecules and metal surface is believed to be the most responsible factor in showing the efficacious corrosion-resistant properties of mild steel in corrosive environments [21].

In this context, a blended extract of *Ageratum houstonianum* and *Chromolaena odorata* leaves (AHL-COL) is exploited as a blended phyto-inhibitor in the present work for controlling the RS corrosion in ConC. Two alien plant species, among 40 species of the genus *Ageratum* in Nepal, are *Ageratum houstonianum* and *Ageratum conyzoides* [22]. Much work has been reported on the *Ageratum conyzoides* extract compared with the *Ageratum houstonianum* species. The aqueous extract of *Ageratum conyzoides* functioned as an anti-corrosive agent for preventing metallic degradation in aggressive electrolytes [23]. Previous work screened out the presence of some phyto-compounds (i.e., phenols, alkaloids, tannins, saponins, steroids, terpenes, and flavonoids) in the leaf extract of *Ageratum conyzoides* [24]. These findings highlighted the plant's rich profile of phyto-compounds and its potential for use in corrosion control applications [25].

The *Ageratum houstonianum* is a flowering shrub belonging to the Asteraceae family, and is an undesirable plants [26]. If people do not manage such unwanted plant, it creates adverse effects in agricultural production sectors. Thus, this study hypothesizes that the leaves of the unwanted *Ageratum houstonianum* can serve as practical and effective green corrosion inhibitors for mitigating the significant corrosion of various metals and alloys in aggressive electrolytes. It might be good for nature, farmers, and the public. In recent years, very few researchers have investigated the anti-corrosive properties of *Ageratum houstonianum* extract on SS-410 steel sheet in 0.5 M H_2SO_4. A corrosion inhibition efficiency of 93% was confirmed for SS-410 stainless steel in 0.5 M H_2SO_4 with 500 ppm *Ageratum houstonianum* extract from electrochemical and weight loss analysis [27].

Comparably, *Chromolaena odorata* (Siam weed and *Banmaraa* in Nepali) is a rapidly growing perennial flowering shrub species of the Asteraceae family, and it is also one of the alien plant species that harm the biodiversity of Nepal [28]. In literature, the ethanol extracts of *Chromolaena odorata* leaf extracts have been noted as an efficacious inhibitor for controlling steel corrosion in aqueous electrolytes [29]. In recent years, studies have reported that individual leaf extracts from both *Ageratum houstonianum* (AHL) and *Chromolaena odorata* (COL) have shown effective anticorrosive properties for mild steel in reinforced concrete, as per the ASTM C876-22b standard [30]. In particular, the addition of 2000-4000 ppm of each AHL or COL extract demonstrated superior corrosion-inhibiting properties than the RC slab without the plant extract [31].

In this context, the present study investigated the synergistic effects of blended extracts of both plant leaves (AHL-COL) for inhibiting the reinforcing mild steel corrosion in concrete using the half-cell potential method. The novelty of this work is that no other research has used the blended extract of both the *Ageratum houstonianum* and *Chromolaena odorata* leaves (AHL-COL) for the first time as green inhibitor against RMS in alkaline concrete composite. This research work recommends the possibility of the consequences of a practical blended plant-based corrosion inhibitor for the prolongation of the RC infrastructures.

2 Materials and Methods

Fresh, uninfected, and healthy leaves of *Ageratum houstonianum* and *Chromolaena odorata* plants were separately collected from the Sunawal area (27.6008° N, 83.6989° E) of Nawalparasi district, Nepal, as described elsewhere [31]. Both the collected plant species were identified as *Chromolaena odorata* L. (Siam weed or *Banmaraa* in Nepali) and *Ageratum houstonianum* Mill (Blue billygoat in English or *Bukejhar* in Nepali). Both plant species identified by the National Herbarium and Plant Laboratory, Plant Department, Godabari, Lalitpur, have their voucher numbers deposited at the office. The fresh leaves of these two plants were dried by placing them in a shaded area for a few weeks.

The air-dried leaves of both plants were separately pulverized for making plant powder, and stored in airtight plastic containers for extract preparation, as noticed in Figure 1(a). Two hundred grams of each plant powder were dipped in 400 mL of methanol for three weeks with regular stirring and filtered the phyto-bioactive solution using a Whatman filter [Figure 1(b)]. The filtrate solution was concentrated with a rotary evaporator [Figure 1(c)] to obtain a solid plant extract [Figure 1(d)].

Fig. 1. Freash leaves of *A. houtonianum* and *C. Odorata* plants and their dried powder (a), the powder soaked with methanol (b), a rotary evaporator machine (c) for the preparation of solid leaf extract (d).

The extract was kept inside a freezer at 4°C until used as an anti-corrosive additive in a concrete composite. The characteristic functional groups of both the plant extracts were ascertained from the FTIR and UV-Visible (SPECORD®200 PLUS, Germany) spectroscopic analysis. The phytochemical screening tests of the extract were conducted to confirm the presence of various phyto-molecules in the extract.

A rust-free thermo-mechanically treated (TMT) and corrugated 500 XD mild steel (MS) rod having a 12 mm diameter with a 300 mm long mild steel rod was reinforced in a concrete beam, as displayed in Figure 2(a). The chemical compositions of the mild steel rod are (wt. %), Fe (>98%) with impurities of C (0.17 to 0.25%), Si (0.4%), Mn (0.9%), S (0.05%), and P (0.05%) [32].

The reinforced concrete (RC) beam with 320 mm × 80 mm × 80 mm dimensions was fabricated using a concrete composite paste (Figure 2a). The concrete paste was prepared by mixing coarse gravel, fine river sand, and ordinary Portland cement (53 grades) powder in a 3:2:1 mass ratio, adding required amount of distilled water with 500 ppm-2000 ppm AHL-COL, as approved by the ASTM C1582/C1582M-11 standard [33]. The cement-water ratio was adjusted to about 0.45.

A total of four rectangular concrete beams were made with the control condition, 500 ppm, 1000 ppm, and 2000 ppm blended AHL-COL, using a rectangular casting box [Figure 2(c)]. The blended AHL-COL extract is a mixture of equi-amounts of the AHL and COL extracts. Additionally, the other eight beams were constructed using a concrete composite paste with AHL and COL at concentrations of 500 ppm, 1000 ppm, 2000 ppm, and 4000 ppm, respectively. About 20 mm of the RMS rod was exposed to one side of the concrete beam, and the equidistant four points (marked as 1, 2, 3, 4) were selected on the beam surface for the recording of the Ecorr, as illustrated in Figure 2(d).

After the preparation of the concrete beams, the E_{corr} of each of the four points was recorded at regular time intervals up to six months or more with the help of a digital multimeter (UNI-T Business, Hong Kong). The exposed end of the RS acted as the working electrode, which was attached to the +ve terminal of the multimeter. A reference electrode was connected to the −ve terminal of the multimeter, as demonstrated in Figure 2(d).

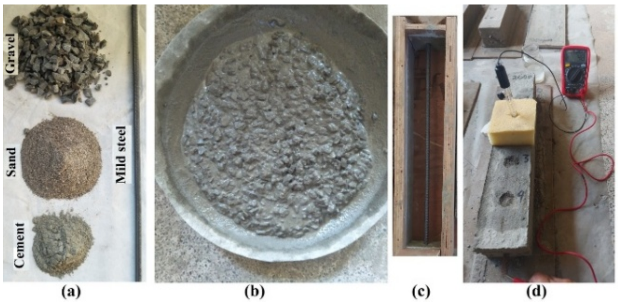

Fig. 2. Pictures of (a) materials of concrete nano-composite mixture and mild steel rod (a), concrete paste (b), fixed steel rod in a casting box (c), and corrosion potential measurement by a digital multi-meter (d).

The average E_{corr} of the four points of each concrete beam was taken for grading three corrosion probability conditions (PC_{corr}) of the RC beam, as approved by the ASTM C876-22b standard [32], which is summarized in Table 1. In this grading system, the average E_{corr} value is regarded as the indicator of the PC_{corr} of the RC beam. For example, if the noted E_{corr} value of the RMS in concrete locates more in a positive than −0.125 V (SCE), the reinforced concrete infrastructure is supposed to be beneath 10% corrosion risk (BCR<10) condition. In contrast, the RC could be rated as an above 90% corrosion risk (ACR>90) when the recorded E_{corr} value of the RMS is negative than, i.e., less than −0.276 V against SCE. It is believed that the RMS is an intermediate corrosion risk (ICR10-90) when the E_{corr} value is in between the BCR<10 and ACR>90 regions (i.e., −0.276 V to −0.176 V), as summarized in Table 1.

Optical images of the RMS surfaces before and after exposure to the extract-treated concrete composite paste were captured for surface analysis using a digital optical microscope. Additionally, the surface sensitive SEM/EDS technique was used to observe the changes in morphology and chemical composition of the RMS surface after exposure to ConC with varying plant concentrations.

Table 1. Average E_{corr} dependent corrosion probability condition (PC_{corr}) of the RMS in concrete beam, as approved by the ASTM C876-22b Standard [32].

Average E_{corr} (V vs SCE)	**PC_{corr} of RMS in concrete beam**
More negative than −0.126	Beneath 10% corrosion risk (BCR<10)
Between −0.276 to −0.126	Intermediate corrosion risk (ICR10-90)
More negative than −0.276	Above 90% corrosion risk (ACR>90)

3 Results and Discussion

For the approximate analysis of the methanol extract from both plants, an UV-visible spectrophotometer (SPECORD® 200 PLUS, Germany) was used to examine the extract under both UV and visible light, covering a wavelength range of 200-800 nm. This method effectively indicates the presence of π-bonding, σ-bonding, lone pairs of electrons, aromatic rings, and chromophores that are characteristic of the phyto-molecules in the analyzed plant extracts, as illustrated in Figure 3.

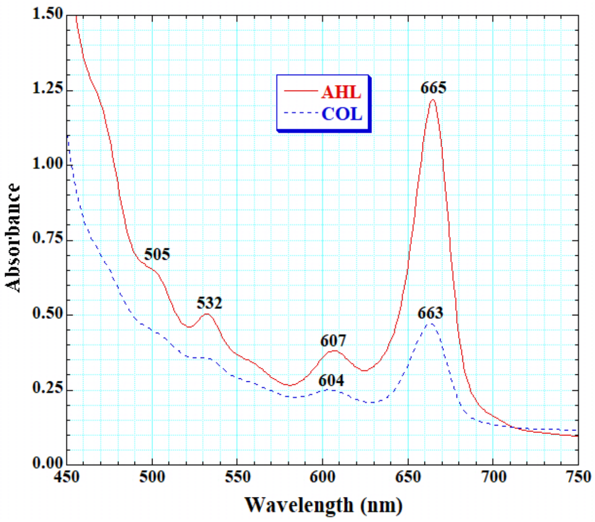

Fig. 3. Recorded UV-Visible spectra of AHL and COL.

The presence of these electronic states, lone pairs of electrons, and aromatic rings is assumed to be effective in controlling the corrosion of reinforcing metals in concrete mix. Results proclaimed the presence of four or more absorption peaks between 450 and 700 nm wavelengths in both plant extracts. The maxima at 505, 532, 607, and 665 nm for the AHL specimen and at 532, 604, and 663 nm for the COL specimen are the characteristics of some phytomolecules as reported in the literature [34]. The UV-Vis spectrophotometry study indicates the presence of secondary metabolites. Nevertheless, analysis of the complex nature of the methanol extracts of both plants using UV-Vis spectroscopy has some disadvantages [35]. Thus, the UV-Vis findings are supplemented by more reliable and pertinent analytical techniques of FTIR and GC-MS for the identification of secondary metabolites in plant-based extracts.

As illustrated in Figure 4, the FTIR absorption peak around 3345-3334 cm^{-1} is owing to O-H stretching vibration of hydrogen bonding [36], and around 2941-2927 cm^{-1} and 2856-2833 cm^{-1} are asymmetrical and symmetrical C-H stretch, respectively [37]. A broad and weak peak around 1720 cm^{-1} appears only in the AHL extract, which indicates the presence of either the N-containing or C=O group or both [36] in the methanol leaf extract of *Ageratum houstonianum*. The appearance of a strong peak around 1638-1616 cm^{-1} for both the plant extracts, and a very intense peak at 1505 cm^{-1} for AHL only indicates the presence of the C=O group in an aromatic ring compound [37].

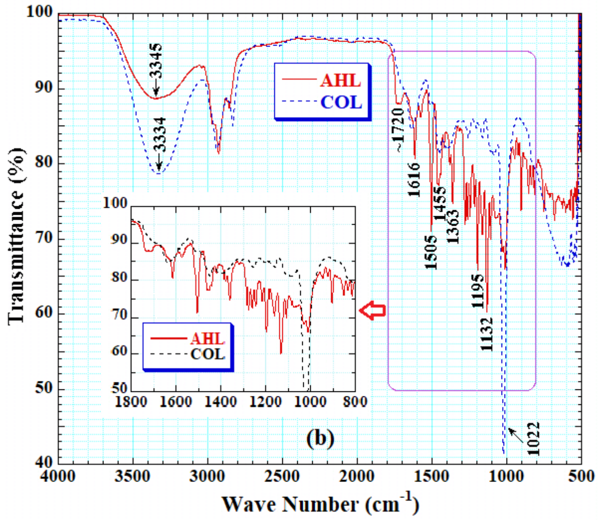

Fig. 4. FTIR spectra of AHL and COL.

Table 2. Assignment of the functional groups present in the AHL and COL extracts.

Wavenumber (cm^{-1})		**Functional group**	**Ref.**
AHL	COL		
3345 (b)	3334 (b)	O–H stretching due to H bonding	[36]
2927 (s)	2941 (s)	C–H (CH_2) asymmetric stretching	[37]
2856 (w)	2833 (w)	C–H (CH_3) symmetrical stretching	[37]
1720 (bw)	–	C–N stretching, C=O group	[36]
1616 (s)	1638 (s)	Aromatic C=C / C=O stretching	[42]
1577 (bw)	–	C–O vibration / aromatic C=C stretching	
1505 (vs)	1515 (vw)	Aromatic C=O stretching	[38]
1455 (s)	1449 (w)	C–H stretching/ aromatic C=C stretching	[39]
1421 (vw)	1400 (bw)	C–H bending	[40]
1363 (s)	–	Aromatic C=C stretching	[42]
1260 (w)	1257 (w)	C–O stretching of organic acids	[43]
1195 (vs)	1205 (vw)	Presence of –COOH group	[44]
1162 (s)	1162 (w)	C–H stretching	[39]
1132 (vs)	1102 (vw)		
1076 (vw)	1087 (w)	C–O ether stretching vibration	[45]
1016 (w)	1022 (vs)	O–H, C–H in plane bending of aromatics	[10]

Besides these diagnostic regions of the FTIR spectra, both AHL and COL extracts have absorption peaks in fingerprint regions of the spectra between 600-1400 cm^{-1} wave numbers, as summarized in Table 2. Peculiarly, the peak value at 1363 cm^{-1} for the AHL extract is probably due to the C=C stretches in the aromatic compounds [42]. These results confirm that both the leaf extracts of AHL and COL are enriched with anti-corrosive aromatic phyto-molecules, constituting hetero-elements such as O, N, and S. Consequently, a consolidated adsorption layer could be easily formed on the RMS surface, resulting from the delocalization of electrons between the more electronegative hetero-elements and the corroded metal surfaces [42].

The phytochemical screening test confirms the presence (+) or absence (−) of various secondary metabolites in the methanol leaf extracts of both AHL and COL, as summarized in Table 3. Alkaloids, flavonoids, phenols, steroids, saponins, and tannins are major secondary metabolites that can favor the development of a corrosion-resistant adsorbed layer between the mild steel and concrete composite. Meanwhile, the AHL showed negative tests for glycosides and carbohydrates in contrast with a positive test for the COL (Table 3).

The COL shows a negative test for terpenoids in contrast to the positive test for the AHL. Despite such experimental observations, previous tests reported that the terpenoid was also present in the leaf extract of the *Chromolaena odorata* plant [46]. The results of the secondary metabolite tests are almost congruous with the prior screening test reports on AHL [47] and COL [48] extracts. The configuration of these phyto-compounds in both the AHL and COL extracts, which are composed of heterogeneous organic molecules containing N, O, S, and aromatic ring compounds in their molecular structures, is the most responsible factor for the adsorption of the molecules onto the surface of corroded metal [49]. Hence, a mixture of AHL and COL (i.e., AHL-COL) extracts could be an effective inhibitor to control the corrosion of reinforcing metal in concrete structures.

Table 3. Results of screening tests for phyto-compounds present in AHL), and COL.

Tests	Phyto-compounds	AHL	COL
Dragendroff's	Alkaloids	+	+
Alkaline reagent	Flavonoids	+	+
Lead acetate	Phenols	+	+
Legal test	Glycosides	−	+
Salkowski	Terpenoids	+	−
Liebermann-Burchard	Steroids	+	+
Foam	Saponins	+	+
Ferric chloride	Tannins	+	+
Molisch's	Carbohydrates	−	+

Researching plant-based phyto-compounds as anti-corrosive additives in ConC would benefit concrete technologists, structural engineers, and corrosion scientists [50]. The plant-based extracts have an impact on extending the stability, reliability, and longevity of the reinforced concrete frameworks. Large amounts of concrete frameworks have faced the problems of unavoidable and unwanted corrosion phenomena of steel/metal embedded in concrete infrastructures.

To avoid such unexpectedly corrosive degradation of the steel/metal in concrete frameworks, an *in situ* electrochemical corrosion potential (E_{corr}) recording would be a conclusive, reliable, and cost- effective method to monitor different corrosion conditions (i.e., BCR<10, ICR10-90, and ACR>90) of the concrete infrastructures at regular intervals of time, as summarized above in Table 1.

Therefore, this study focused on observing the inhibitory effects of various concentrations of blended AHL-COL extract added in ConC to control CoS corrosion. We measured the corrosion potential (E_{corr}) at four points on each concrete beam over a period of up to six months, using the half-cell potential measurement method, and the results are illustrated in Figure 5. The figure demonstrates the changes in the E_{corr} of four surface-points (i.e., Pt-1, Pt-2, Pt-3, Pt-4) of the RMS in all four concrete beams with exposure time up to six months or more, which were made ready the concrete beam using the control ConC without the addition of the blended plant extract [Figure 5(a)], and by the inclusions of 500 ppm [Figure 5(b)], 1000 ppm [Figure 5(c)], and 2000 ppm [Figure 5(d)] AHL-COL extract in the ConC.

The E_{corr} value of the RC beams with different concentrations of the AHL-COL extract has been shifted towards a region of less than 10% corrosion probability (P_{corr}) after exposure to the RC beams between 15 and 180 days or more at ambient conditions, except the control RC beam. The E_{corr} value of all four points of the control RC beam without the addition of plant extract is shifted to a noble potential region by increasing the exposure time to about one month [Figure 5(a)]. However, with increasing the exposure times about one to three months, the E_{corr} of the control concrete beam has moved remarkably towards an intermediate corrosion risk (i.e., ICR10-90) region, and ultimately attained a steady state E_{corr} less noble than −0.275 V (SCE) during the exposure between 3 to 6 months or more, inferring a high corrosion risk of the RMS in the concrete beam without the plant extract.

The results revealed that the 500, 1000, and 2000 ppm AHL-COL improved the anti-corrosive properties of the ConC. Probably, a stable film formed on the RMS surface by the process of physical or chemical adsorption of phyto-compounds extracted from the plant-based extract [4]. The film prevents corrosive ions or molecules from entering the steel surface through the concrete nano-pores, as previously stated [51].

Besides, the variation of the E_{corr} with exposure time of the concrete beams with different concentrations of the blended AHL-COL extract is found to be time-dependent, as reported in previous studies [52]. The structure of the concrete beams with the AHL-COL extract should be denser through a high degree of hydration and low porosity at long exposure times, and hence decrease the diffusion coefficient of pollutant ions/molecules across the interfacial region of the concrete nano-matrix and reinforced metal surface. However, such phenomena should not be moved ahead in the case of the beam without the blended extract. Thence, the E_{corr} of the concrete beam without plant extract shifted to a less noble direction with time, as demonstrated in Figure 5(a).

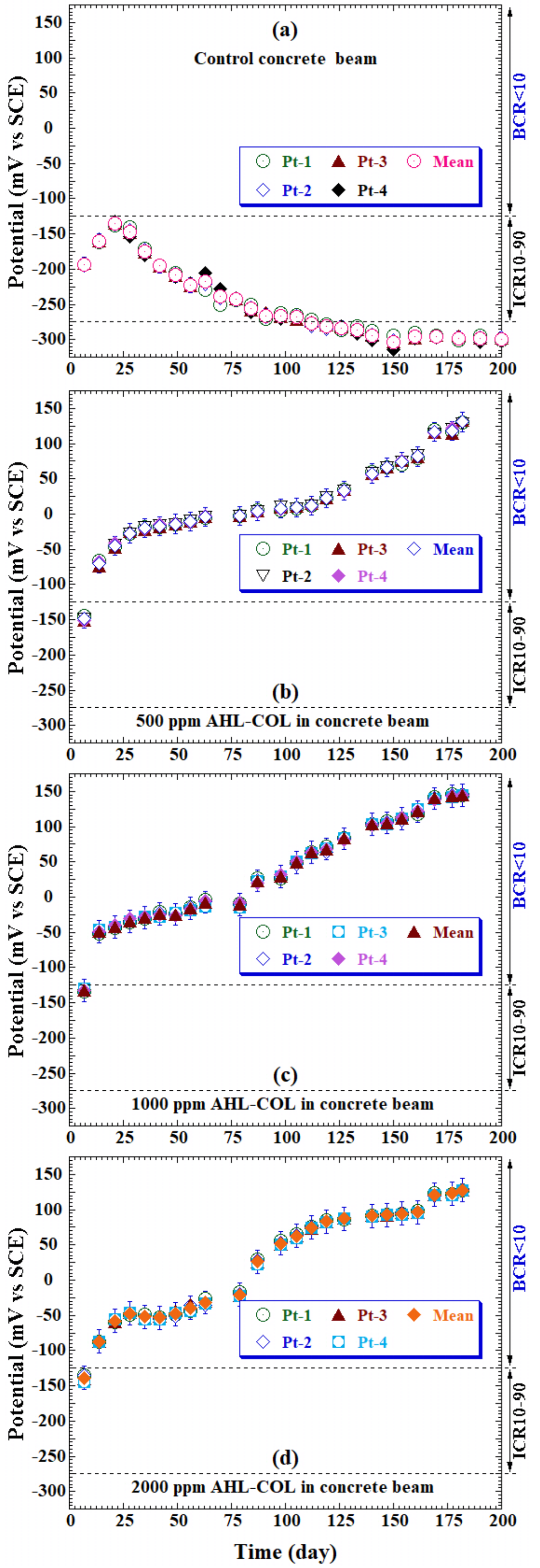

Fig. 5. The changes of electrochemical corrosion potential of the RMS in concrete beam at (a) control condition and with the additions of (b) 500 ppm (c) 1000 ppm and (d) 2000 ppm AHL-COL in concrete composite, as a function of exposure time at ambient atmosphere.

Additionally, Figure 6(a) summarizes the variation of the average E_{corr} values for all four points on each concrete beam, including standard error bars. As the exposure time increases, the average E_{corr} shifts to a more corrosion-resistant region (i.e., where BCR < 10), moving away from intermediate corrosion risk areas. A more stable protective layer is expected to form on the surface of the RMS in the presence of heterogeneous organic molecules containing N, O, S, and aromatic ring compounds. Also, it gives a meaningful indication that the standard deviation from the average E_{corr} is < 10 mV except in very few cases (<2%).

The outcomes revealed that localized corrosion of the RMS in ConC beam could not be expected with the additions of both plant extracts and their blended extracts. The phyto-compounds of the plant extract enhanced to form an anti-corrosive passive film across the interface between the mild steel and concrete matrix, which shifts the corrosion condition from the region of the intermediate corrosion to a region with less than < 10% chance of corrosion occurrence [30].

Furthermore, Figures 6(b), 6(c), and 6(d) illustrate the variation with the average E_{corr} of the RMS in concrete beams without (control) and with different concentrations of the plant-based three types of extracts (i.e., AHL, COL, blended AHL-COL). The motive of the study is to compare the inhibitory effects of the blended AHL-COL concentrations over the individual AHL or COL extract in preventing the corrosion of the RMS in the ConC. The same trend in the change of the average E_{corr} of the concrete beams with 500 to 2000 ppm AHL-COL, AHL, or COL is observed. However, the additions of 500-2000 ppm AHL-COL in the concrete beam showed significantly higher corrosion-inhibiting ability and expected high passivity strength compared with the concrete beams with the same concentrations of the individual AHL or COL extract. Consequently, it can be stated that the blended AHL-COL demonstrated a synergistic effect in inhibiting the corrosion of mild steel in the ConC.

The surface features of the embedded mild steel before and after reinforced in concrete composite (ConC) at control condition and with different concentrations of the blended HL-COL extract was also investigated from the recorded optical images of the sample specimens (Figure 7). The corrugated mild steel surface before reinforcement in concrete composite exhibits comparatively a smooth surface without notable defects, as shown in Figure 7(a).

In contrast, an optical image of the RMS surface, which was exposed in the control ConC, disclosed that the corrosion product has remarkably appeared on the metal surface compared to the optical images of the exposed sample specimens in a concrete with different concentrations of AHL-COL extract for about six months, as displayed in Figure 7(b). The images of the RMS surface in the concrete beam with 1000 ppm and 2000 ppm AHL-COL extracts are smooth without significant rust defects, as noticed in Figures 7(c), and 7(d). The E_{corr} results, as described above in Figs. 6 and 7, established the fact that the plant-based protective layers are successfully developed over the RMS surface after exposure to the ConC for long periods in the ambient atmosphere by adsorbing/interacting with the conjugated polar groups of the phyto-compounds on the RMS surface, which have sufficient electrophilic centers [53].

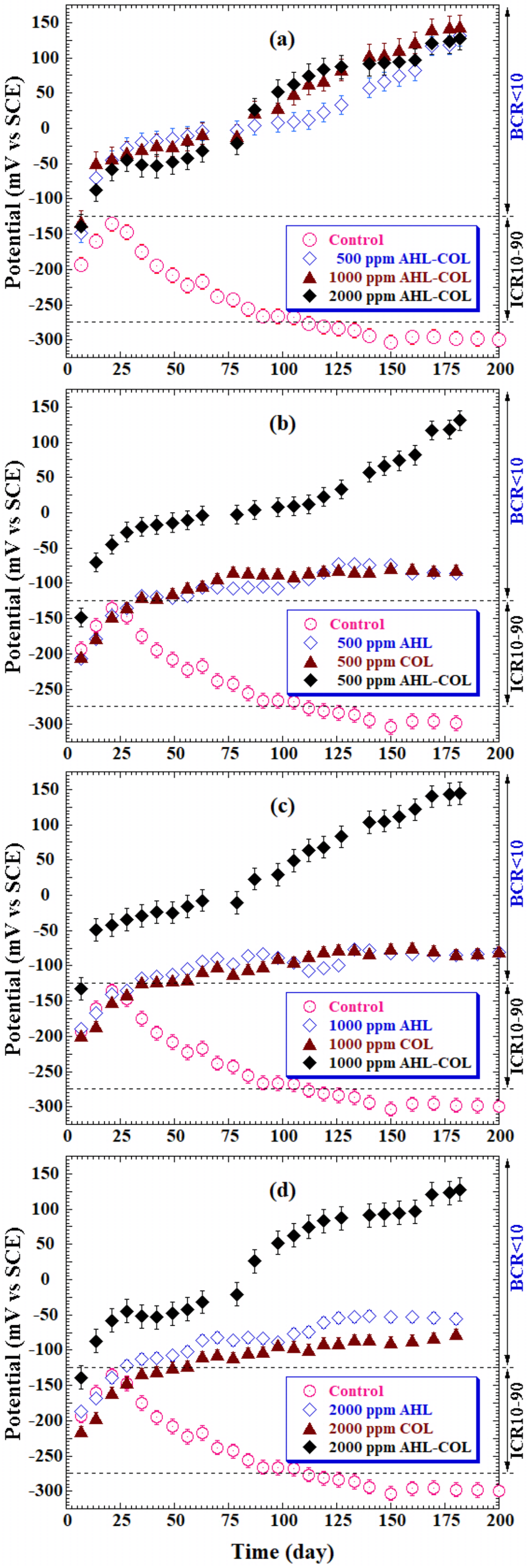

Fig. 6. Variation of the average corrosion potential of RMS in concrete beam with various concentrations of AHL-COL in concrete composite.

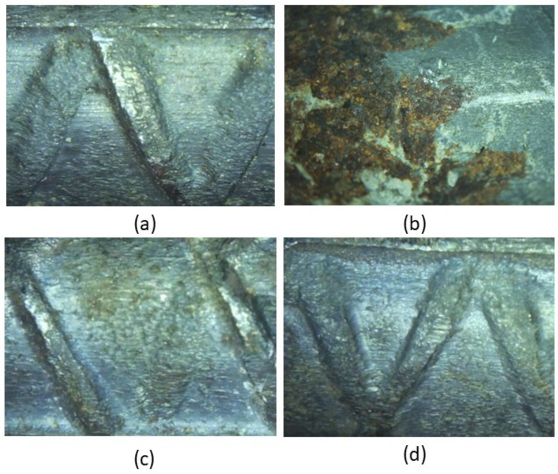

Fig. 7. Optical images of the mild steel (a) before, and after embedding in concrete composite (b) without plant extract, (c) with 1000 ppm AHL-COL, and (d) with 2000 ppm AHL-COL.

Accordingly, the RMS corrosion rate would progressively decline upon the addition of different amounts of the blended AHL-COL extract in ConC. It indicates the formation of a passive layer over the RMS surface in the concrete composite with blended extracts. Moreover, the morphological features and chemical compositions of the corroded RMS surface were investigated after exposing the sample specimens for six months or more in ConC using a scanning electron microscope (SEM) with an energy-dispersive X-ray (EDX) spectrometer. The results of the SEM/EDX analysis provide solid evidence supporting the relationship between E_{corr} variation and the corrosion-inhibiting efficiency of the RMS in ConS. This relationship highlights the impact on electrochemical potential values and identifies the areas at risk of corrosion. SEM images reveal that irregular rusting occurs on the surface of the RMS, which has crumbled into small fragments on the corroded surfaces of the reinforcing materials, as illustrated in Figure 8(a).

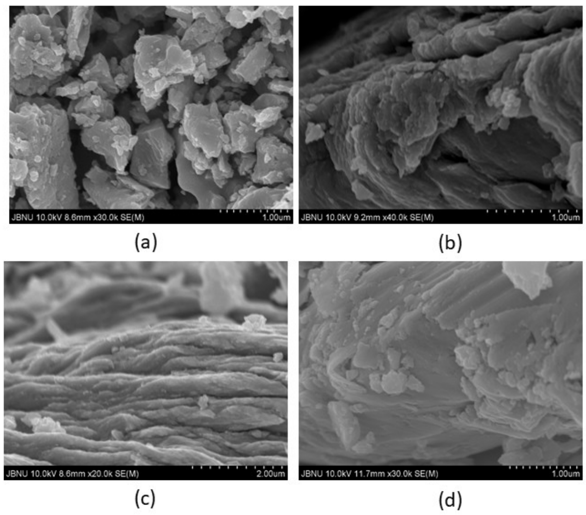

Fig. 8. SEM images of the RMS after reinforcing it for about six months in concrete composite (a) without extract (control), and with extracts of (b) 2000 ppm AHL, (c) 1000 ppm AHL-COL, and (d) 2000 ppm AHL-COL.

However, additions of 1000 ppm and 2000 ppm AHL-COL, including 2000 ppm AHL to the concrete composite, lower the possibility percentage of the RMS corrosion risk. The SEM image clearly shows that the corrosion-related surface imperfections are eliminated on the inhibited mild steel surface, demonstrating the increased inhibition efficacy of three different extracts, as in Figuers 8(b), 8(c) and 8(d). The RMS corrosion is controlled through the adsorption mechanism. Hence, the additions of 1000-2000 ppm AHL-COL lower the possibility of corrosion risk of the reinforcing concrete infrastructures, which is also supported by the results of the EDX analysis, as demonstrated in Figure 9.

EDS analysis reveals significant amounts of carbon and oxygen on the RMS surface after being embedded in the concrete mix under control conditions, as shown in Figure 9(a). Nevertheless, the amount of Fe on the corroded RMS surface is remarkably lower compared with the composition of the fresh mild steel rod (i.e., >98%). Such changes in the chemical components of the RMS surface in the control ConC reveal the formation of corrosion products of the iron oxide layer on the corroded steel surface [54].

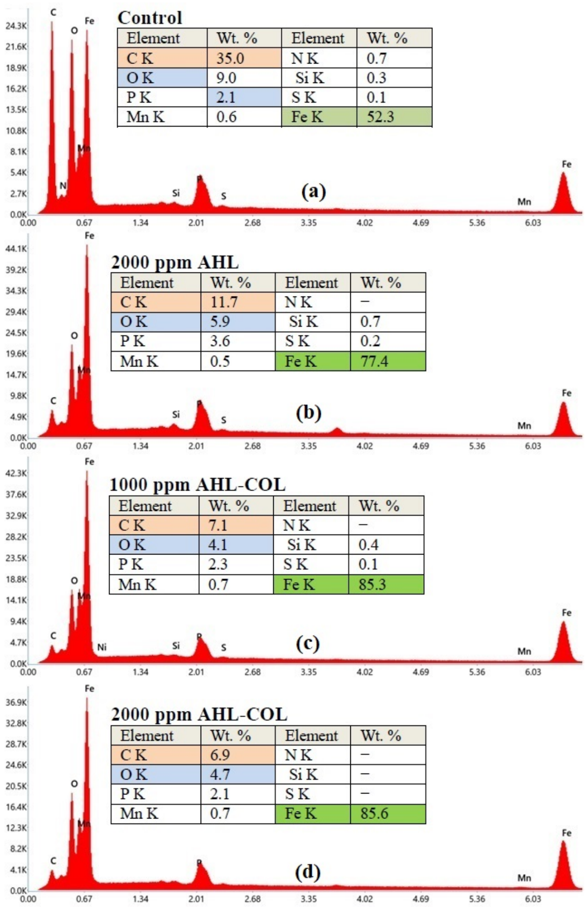

Fig. 9. EDX analysis of the RMS surfaces after exposed for six months in concrete composite (a) at control condition, and with blended (b) 1000 ppm AHL, (c) 1000 ppm AHL-COL and (d) 2000 ppm AHL-COL extracts.

When the RMS is exposed in concret beam with only 2000 ppm AHL and blended 1000-2000 ppm AHL-COL extracts, as shown in Figures 9(b), 9(c), and 9(d), respectively, the EDX spectrum shows comparatively lower oxygen and higher percentages of Fe, showing low corrosion risk on the RMS with the addition of the AHL or the blended AHL-COL extracts in the ConC. As a result, the formation of a protective thin oxide layer by the addition of AHL and AHL-COL extracts in the CNC enhances the anti-corrosive properties [55]. Among these three extracts, the blended two extracts (i.e., 1000 ppm & 2000 ppm AHL-COL) have shown better anti-corrosive behavior of the RMS in the concrete beam.

4 Conclusion

Based on the screening test, FTIR, UV-Vis spectroscopy, half-cell potential, and surface analysis, the experimental findings support the development of a novel plant-based concrete additive for the corrosion control of the RMS in the reinforced concrete beams. The blended extracts of *Ageratum houstonianu*m and *Chromolaena odorata* at concentrations of 500 ppm, 1000 ppm, and 2000 ppm exhibit a synergistic effect in inhibiting the corrosion of RMS in the reinforced concrete beam. It is primarily due to the formation of a compacte adsorption layer on the surfaces of the RMS.

The consequences of this work would be a breakthrough in understanding the knowledge on AHL-COL extract as noble green corrosion inhibitor for extending the lifespan of the RMS in concrete structures. The results of the present work permit the production of plant-based novel anti-corrosive concrete additives on a commercial scale to control SRC corrosion. A detailed study on the film formation mechanism using electrochemical impedance spectroscopy (EIS), linear polarization, and other relevant surface analysis techniques.

This research work was supported by the University Grants Commission (UGC) of Nepal under the Ph. D. Fellowship and Research Support No.: PhD-78/79-S&T-03 to author MG. The authors acknowledge Dr. Ishwor Pathak of Jeonbuk National University, South Korea, for providing SEM-EDS facilities.

References

[1] I. Marcos, J.-T. San-José, L. Garmendia, A. Santamaría, J.M. Manso, Central lessons from the historical analysis of 24 reinforced-concrete structures in northern Spain. *J. Cult. Heritage*. **20**, 649–659 (2016). https://doi.org/10.1016/j.culher.2016.03.003

[2] Y.P. Asmara, T. Kurniawan, A.G.E. Sutjipto, J. Jafar, Application of plants extracts as green corrosion inhibitors for steel in concrete- a review. *Indonesian J. Sci. Technol.* **3**(2), 158–170 (2018).

[3] A. Biparva, *Reinforced Concrete Corrosion: A Silent Killer*, (2016). https://www.constructioncanada.net/reinforced-concrete-corrosion-a-silent-killer

[4] G. Venkatesh, C. Kamal, P. Vennila, S. Kaya, M.G.L. Annaamalai, B.E. Ibrahimi, Sustainable corrosion inhibitor for steel embedded in concrete by Guar Gum: Electrochemical and theoretical analyses. *Appl. Surf. Sci. Adv.* **12**, 100328 (2022).

[5] S. Robuschi, A. Tengattini, J. Dijkstra, I. Fernandez, K. Lundgren, A closer look at corrosion of steel reinforcement bars in concrete using 3D neutron and X-ray computed tomography. *Cem. Conc. Res.* **144**, 106439 (2021).

[6] U.M. Angst, Challenges and opportunities in corrosion of steel in concrete. *Mater. Struct.* **51**(1), 4 (2018).

[7] M. Oki, S.A. Akintola, A.A. Adediran, P.P. Ikubanni, B.T. Ogunsemi, Reinforcement bar corrosion - causes and management. *J. Phys.: Conf. Ser.* **1378**(2), 022095 (2019).

[8] E.S.J. Ahmed, G.M. Ganesh, A comprehensive overview on corrosion in RCC and its prevention using various green corrosion inhibitors. *Buildings.* **12**(10), 1682 (2022).

[9] S. Ghoreishiamiri, P.B. Raja, M. Ismail, S.F.H. Karouei, P. Forouzani. *Areca catechu*: an eco-friendly corrosion inhibitor for reinforced concrete structures in corrosive medium. *J. Bio-Tribo-Corros.* **7**, 22 (2021).

[10] J. Bhattarai, M. Somai, N. Acharya, A. Giri, A. Roka, N.P. Phulara, Study on the effects of green-based plant extracts and water-proofers as anti-corrosion agents for steel-reinforced concrete slabs. *E3S Web Conf.* **302**, 02018 (2021).

[11] B. Valdez-Salas, R. Vazquez-Delgado, J. Salvador-Carlos, E. Beltran-Partida, R. Salinas-Martinez, N. Cheng, M. Curiel-Alvarez, *Azadirachta indica* leaf extract as green corrosion inhibitor for reinforced concrete structures: corrosion effectiveness against commercial corrosion inhibitors and concrete integrity. *Materials.* **14**(12), 3326 (2021).

[12] R. Anitha, S. Chitra, V. Hemapriya, I. Chung, S. Kim, M. Prabakaran, Implications of eco-addition inhibitor to mitigate corrosion in reinforced steel embedded in concrete. *Constr. Build. Mater.* **213**, 246–256 (2019).

[13] B.E.R. Amitha, B.B.J. Basu, Green corrosion inhibitors for corrosion protection of metals and alloys: an overview. *Int. J. Corros.* **2012**, 1–15 (2012).

[14] N. Patni, S. Agrawal, P. Shah, Greener approach towards corrosion inhibition. *Chin. J. Eng.* **2013**, 784186 (2013).

[15] S.Z. Salleh, A.H. Yusoff, S.K. Zakaria, M.A.A. Taib, A. Abu Seman, M.N. Masri, M. Mohamad, S. Mamat, S. Ahmad Sobri, A. Ali, P.T. Teo, Plant extracts as green corrosion inhibitor for ferrous metal alloys: a review. *J. Cleaner Prod.* **304**,127030 (2021).

[16] I.B. Onyeachu, D.I. Njoku, S.C. Nwanonenyi, C.C. Ahanotu, K.M. Etiowo, Investigation into the adsorption and inhibition properties of sodium octanoate against CO_2 corrosion of C1018 carbon steel under static and hydrodynamic conditions. *Sci. Afr.* **20**, e01603 (2023).

[17] R. Naderi, A. Bautista, F. Velasco, M. Soleimani, M. Pourfath, Use of licorice plant extract for controlling corrosion of steel rebar in chloride-polluted concrete pore solution. *J. Mol. Liq.* **346**, 117856 (2022).

[18] Q. Wang, X. Wu, H. Zheng, L. Liu, Q. Zhang, A. Zhang, Z. Yan, Y. Sun, Z. Li, X. Li, Evaluation for *Fatsia japonica* leaves extract as green corrosion inhibitor for carbon steel in simulated concrete pore solutions. *J. Buil. Eng.* **63**, 105568 (2023).

[19] R. Naderi, A. Bautista, F. Velasco, M. Soleimani, M. Pourfath, Green corrosion inhibition for carbon steel reinforcement in chloride-polluted simulated concrete pore solution using *Urtica dioica* extract. *J. Buil. Eng.* **58**, 105055 (2022).

[20] Q. Liu, Z. Song, H. Han, S. Donkor, L. Jiang, W. Wang, H. Chu, A novel green reinforcement corrosion inhibitor extracted from waste *Platanus acerifolia* leaves. *Constr. Buil. Mater.* **260**, 119695 (2020).

[21] C. Verma, E.E. Ebenso, M. Quraishi, Ionic liquids as green and sustainable corrosion inhibitors for metals and alloys: An overview, *J. Mol. Liq.* **233**, 403–414 (2017).

[22] P. Satyal, A. Poudel, W.N. Setzer, Variation in the volatile phytochemistry of *Ageratum conyzoides*, *Am. J. Essent. Oils Nat. Prod.* **6**, 7–10 (2018).

[23] O.O. Adeyemi, O.O. Olubomehin, R.O. Bello, Investigation of *Ageratum conyzoides* aqueous extract as inhibitor for hydrochloric acid corrosion of SX 316 steel. *Acad. J. Sci. Eng.* **8**(1), 20–32 (2022).

[24] R. Chahal, A. Nanda, E.K. Akkol, E. Sobarzo-Sánchez, A. Arya, D. Kaushik, R. Dutt, R. Bhardwaj, M.H. Rahman, V. Mittal, *Ageratum conyzoides* L. and its secondary metabolites in the management of different fungal pathogens. *Molecules (Basel, Switzerland)*. **26**(10), 2933 (2021).

[25] C.A. Coy-Barrera, L.D. Becerra, S.A. Torres-Cortés, V.C. Gonzalez, Eco-friendly corrosion inhibition study of croton extracts (Euphorbiaceae) for mild steel in HCl 1.0 M: experimental and theoretical studies. *Results Chem.* **16**, 102498 (2025).

[26] A. Lamsal, M.P. Devkota, D.S. Shrestha, S. Joshi, A. Shrestha, Seed germination ecology of *Ageratum houstonianum*: a major invasive weed in Nepal. *Plos One*. **14**(11), e0225430 (2019).

[27] R. Singh, D. Prasad, Z. Safi, N. Wazzan, L. Guo, De-scaling, experimental, DFT, and MD-simulation studies of unwanted growing plant as natural corrosion inhibitor for SS-410 in acid medium. *Colloids Surf. A.* **649**, 129333 (2022).

[28] K.K. Shah, I. Tiwari, S. Tripathi, S. Subash Subedi, J. Shrestha, Invasive alien plant species: A threat to biodiversity and agriculture in Nepal. *Agriways*. **8**(2), 62–73 (2020).

[29] M. M. Muzakir, F.O. Nwosu, S.O. Amusat, Mild steel corrosion inhibition in a NaCl solution by lignin extract of *Chromolaena odorata*. *Port. Electrochim. Acta.* **37**(6) 359–372 (2019).

[30] ASTM C876-22b, *Standard Test Method for Corrosion Potentials of Uncoated Reinforcing Steel in Concrete,* in Annual book of ASTM

standards, ASTM International, West Conshohocken, USA, (2022).

[31] N.K. Pandey, L. Gupta, J. Bhattarai, N.P. Bhattarai, An inhibitory prospect of leaf extracts of flossflower and yam for rebar steel corrosion in concrete aggregates. *E3S Web Conf.* **559**, 02008 (2024).

[32] M. Gautam, D. B. Subedi, J.R. Dhungana, M. Dhakal, K.P. Bohara, N.P. Bhattarai, J. Bhattarai, A sustainable approach for mitigating rebar corrosion in adverse conditions using *Phyllanthus emblica* (L.) leaf extract as concrete scale inhibitor. *Int. J. Corros. Scale Inhib*. **14**(3), 1522-1554 (2025).

[33] ASTM C1582/C1582M-11, *Standard Specification for Admixtures to Inhibit Chloride Induced Corrosion of Reinforcing Steel in Concrete,* in Annual book of ASTM standards, ASTM International, West Conshohocken, USA, (2017), pp. 10.

[34] T.K. Patle, K. Shrivas, R. Kurrey, S. Upadhyay, R. Jangde, R. Chauhan, Phytochemical screening and determination of phenolics and flavonoids in *Dillenia pentagyna* using UV–Vis and FTIR spectroscopy. *Spectrochim. Acta Part A*. **242**, 118717 (2020).

[35] B. Renuka, B. Sanjeev, D. Ranganathan, Evaluation of phyto-constituents of *Caralluma nilagiriana* by FTIR and UV-Vis spectroscopic analysis. *J. Pharmacogn. Phytochem.* **5**(2), 105–108 (2016).

[36] E. Safitri, H. Humaira, N. Nazaruddin, S. Susilawati, M. Murniana, N.D. Md Sani, *Dioscorea alata* L anthocyanin extract methanol as a sensitive pH active compound. *J. Phys.: Conf. Ser.* **1869**, 012058 (2021).

[37] A. Sulistiawan, W. Setyaningsih, A. Rohman, A new FTIR method combined with multivariate data analysis for determining aflatoxins in peanuts (*Arachis hypogaea*). *J. Appl. Pharm. Sci.* **12**(7), 199−206 (2022).

[38] P.P. Yue, Y.J. Hu, G.Q. Fu. C.X. Sun. M.F. Li, F. Peng, R.C. Sun, Structural differences between the lignin-carbohydrate complexes (LCCs) from 2-24 months old bamboo (*Neosinocalamus affinis*). *Int. J. Mol. Sci.* **19**(1), (2018).

[39] A. Inan Genc, S. Gok, S. Banerjee, F. Severcan, Valdecoxib recovers the lipid composition, order and dynamics in colon cancer cell lines independent of COX-2 expression: An ATR-FTIR spectroscopy study. *Appl. Spectrosc.* **71**(1), 105–117 (2017).

[40] J.M. Barcelo, A.M. Gatchallan, I.J.B. Aquino, D.R.E. Ollero, F.L.D. Cortez, T.M. Costales, L.A.Q. Marzo, FTIR spectrum and antimutagenicity of *coffea arabica* pulp and *Arachis hypogaea* test in relation to their *In vitro* antioxidant properties. *Asia Pac. J. Multidiscip. Res*. **3**(4), 99−108 (2015).

[41] U.J. Chukwu, T.O. Uchechukwu, O. Akaranta, Synthesis of new cation exchanger resins from chemically modified peanut (*Arachis hypogaea* L.) testa extract. *Int. J. Sci. Eng. Res.* 8(3), 523−529 (2017).

[42] J.E. Eziuka, I.B. Onyeachu, D.I. Njoku, S.C. Nwanonenyi, M.A. Chidiebere, E.F. Oguzie, *Elucidating the inhibition behaviour of Pterocarpus santalinoides* leaves extract on mild steel corrosion in H_2SO_4 solution–GC-MS, FTIR, SEM, Experimental and computational approach. *Moroccan J. Chem.* **11**(3), 579–593 (20223).

[43] C. Zhang, J. Deng, L. Lin, M. Li, X. Sheng, H. Xia, M. Lin, Use of ATR-FTIR spectroscopy and chemometrics for the variation of active components in different harvesting periods of *Lonicera japonica*. *Int. J. Anal. Chem.* **2022**, 8850914 (2022).

[44] M. Maczka, A. Ciupa, A. Gągor, A. Sieradzki, A. Pikul, B. Macalik, M. Drozd, Perovskite metal formate framework of [NH_2-CH^+-NH_2]Mn($(HCOO)_3$]: phase transition, magnetic, dielectric, and phonon properties. Inorg. Chem. **53**(10), 5260−5268 (2014).

[45] E. Fachriyah, M.A. Ghifari, K. Anam, Isolation, identification, and xanthine oxidase inhibition activity of alkaloid compound from *Peperomia pellucida*. *IOP Conf. Ser.: Mater. Sci. Eng.* **349**, 12017 (2018).

[46] K. Vijayaraghavan, J. Rajkumar, M.A. Seyad, Efficacy of *Chromolaena odorata* leaf extracts for the healing of rat excision wounds. *Vet. Med.* **62**(10), 565–578 (2017).

[47] S.K. Chandraker, M. Lal, M.K. Ghosh, V. Tiwari, T.K. Ghorai, R. Shukla, Green synthesis of copper nanoparticles using leaf extract of *Ageratum houstonianum* Mill. and study of their photocatalytic and antibacterial activities. *Nano Express* **1**(1), 010033 (2020).

[48] F. Odutayo, C. Ezeamagu, T. Kabiawu, D. Aina, G. Mensah-Agyei, Phytochemical screening and antimicrobial activity of *Chromolaena odorata* leaf extract against selected microorganisms. *J. Adv. Med. Pharm. Sci.* **13**(4), 1–9 (2017).

[49] S. Aribo, S.J. Olusegun, L.J. Ibhadiyi, A. Oyetunji, D.O. Folorunso, Green inhibitors for corrosion protection in acidizing oilfield environment. *J. Assoc. Arab Univ. Basic Appl. Sci.* **24**(1), 34–38 (2017).

[50] M. Sheydaei, The use of plant extracts as green corrosion inhibitors: a review. *Surfaces*. **7**(2), 380-403 (2024).

[51] A. Chaouiki, M. Chafiq, Y.G. Ko, A.H. Al-Moubaraki, F.Z. Thari, R. Salghi, K. Karrouchi, K. Bougrin, I.H. Ali, H. Lgaz, Adsorption mechanism of eco-friendly corrosion inhibitors for exceptional corrosion protection of carbon steel: Electrochemical and first-principles DFT evaluations *Metals*. **12**(10), 1598 (2022).

[52] D.V.P. Tran, Time-dependent model for evaluating corrosion potential and electrical resistivity of reinforced concrete. *Eng. J.* **25**(1), 125–135 (2021).

[53] K. Hjouji, E. Ech-chihbi, I. Atemni, M. Ouakki, T. Ainane, M. Taleb, Z. Rais, *Datura stramonium*

plant seed extracts as a new green corrosion inhibitor for mild steel in 1M HCl solution: Experimental and surface characterization studies. *Sustainable Chem. Pharm.* **34**, 101170 (2023).

[54] R. Jalab, A.B. Ali, M. Khaled, M. Abouseada, S. Al-Khalil, A. Al-Suwaidi, S. Hamze, I.H. Hussein, Novel polyepoxysuccinic acid-grafted polyacrylamide as a green corrosion inhibitor for carbon steel in acidic solution. *ACS Omega* **8**(19), 16673–16686 (2023).

[55] D.K. Verma, F. Khan, Green approach to corrosion inhibition of mild steel in hydrochloric acid medium using extract of spirogyra algae. *Green Chem. Lett. Rev.* **9**(1), 52–60 (2016).